Carbohydrate Polymers 99 (2014) 257–263

Contents lists available at ScienceDirect

Carbohydrate Polymers

journal homepage: www.elsevier.com/locate/carbpol

Gelation behavior of *in situ* forming gels based on HPMC and biphasic calcium phosphate nanoparticles

Roghayyeh Marefat Seyedlar, Azizollah Nodehi*, Mohammad Atai, Mohammad Imani

Iran Polymer and Petrochemical Institute (IPPI) , PO Box 14965/115, Tehran, Iran

ARTICLE INFO

Article history:
Received 17 April 2013
Received in revised form 19 June 2013
Accepted 26 July 2013
Available online 14 August 2013

Keywords:
Injectable *in situ* forming gels
Calcium phosphates nanoceramics
Rheological behavior
Hydroxypropyl methylcellulose
Biphasic calcium phosphate

ABSTRACT

In this study, *in situ* forming gels are prepared using biphasic calcium phosphate (BCP) as filler and hydroxypropyl methylcellulose (HPMC) as a matrix exhibiting temperature-sensitive behavior. BCP was composed of β-tricalcium phosphate (β-TCP) with plate-like morphology and nano-sized hyadroxyapatite (HAp). Gel permeation chromatography (GPC) and rheological results showed that low molecular weight HPMC had lower gelation temperature. Effects of BCP content and HAp/β-TCP ratio on rheological behavior of the gels were investigated. According to the results, all samples showed a pseudoplastic behavior and their viscosity increased with increasing mineral phase, especially β-tricalcium phosphate. In order to investigate interaction mechanisms between the mineral phase and polymer and also the effects of ion release, particle size, hydrophobisity, and hydrophilisity, hydrophobic and hydrophilic silica with different particle sizes were also utilized. Results showed that factors affecting the hydrophobisity and hydrophilisity of solution may influence the rheological properties.

1. Introduction

Bone is one of the tissues that most frequently is used for regeneration and transplantation (Link, 2008). Annually many bone grafting operations are performed to treat bone diseases (De Boever, De Boever, & De Vree, 1998; Laurencin, Ambrosio, Borden, & Cooper, 1999; Mickiewicz, 2001; Temenoff & Mikos, 2000). Autografts, allografts, and xenografts are candidates for bone transplantation. The use of allografts and xenografts are limited due to their possible immunological response of the host against graft and the risk of transmission of infectious diseases, whereas autografts are restricted in application by problems related to the low availability of the transplantable tissue, lack of functional shape of the transplant, and leaving painful donor sites (Damien & Parsons, 1991; Link, 2008; Mickiewicz, 2001). To overcome these problems, the uses of synthetic bone substitutes were proposed (Boix et al., 2006; Moore, Graves, & Bain, 2001).

Calcium phosphate ceramics are non-toxic materials suitable for bone tissue engineering owing to their high similarity to biological apatites present in native bones, biocompatibility, and bioactivity. Among them, hydroxyapatite (HAp) and β-tricalcium phosphate (β-TCP) are the most widely used (Boix et al., 2006). HAp is considered as a non-resorbable ceramic due to its stability at physiological conditions and low profile of cellular resorption by osteoblasts, or macrophages, unless when particle size is small enough for phagocytosis. Mechanical properties of HAp are also superior to other calcium phosphate ceramics (Dorozhkin, 2010a; Link, 2008).

Tricalcium phosphate is similar to the amorphous component of bone (Cho, Jung, Han, & Kang, 2009; Kim, 2007; Link, 2008). β-TCP is commonly used in combination with HAp, due to its higher solubility, to balance solubility characteristics of HAp during dissolution and re-precipitation processes occurring *in vivo* (Castellani, Zanoni, Tangl, Van Griensven, & Redl, 2009; Dorozhkin, 2010a). Application of ceramics for treating bone defects suffers highly from their brittleness and difficulty to shape them exactly as the defects (Lee et al., 1999; Yang, Kim, & Ong, 2005). Therefore, they are usually used as composites with biopolymers such as hydrogels, which are able to mimic extracellular matrix characteristics such as hydrophilicity and water retention capability. Combining hydrogels and ceramics into composites can also overcome the weak mechanical properties of hydrogels (Slaughter, Khurshid, Fisher, Khademhosseini, & Peppas, 2009). New materials based on composites of ceramics and the biopolymers have also been developed (Dorozhkin, 2010b; Lee et al., 1999).

Hydroxypropyl methylcellulose (HPMC) is a semi-synthetic cellulose derivative which can form *in situ* forming injectable tissue engineering scaffolds or drug delivery devices. It is also used as polymer phase in bone cements due to non-toxic characteristics and possessing adequate mechanical properties (Escudero, Ferrero, & Jiménez-Castellanos, 2010; Pérez, Wargon, & Pilosof, 2006; Silva et al., 2008; Xu, Weir, Burguera, & Fraser, 2006). HPMC aqueous solutions form reversible gels with increasing

* Corresponding author. Tel.: +9821 48662463; fax: +9821 44580023.
E-mail addresses: a.nodehi@ippi.ac.ir, anodehi@yahoo.com (A. Nodehi).

0144-8617/$ – see front matter © 2013 Elsevier Ltd. All rights reserved.
http://dx.doi.org/10.1016/j.carbpol.2013.07.078

temperature via hydrophobic interactions occurring between hydrophobic segments of the polymer chains, with a lower critical solution temperature (LCST) between 75 and 90 °C, depending on the degree of substitution of hydroxypropyl and methyl functional groups and also on their distribution along the polymer chain [19–21]. The main advantage of injectable tissue engineering scaffolds based on HPMC composite hydrogels is a reduction in the degree of invasiveness of osteoplasty surgery, a shortening of the operation time, homogenous distribution of cells and molecular signals throughout the scaffold, direct injection into cavities with irregular shape and size and finally accessibility to limited or narrow cavities Xu, Weir, & Simon, 2008; Weiss et al., 2005; Zhao, Weir, & Xu, 2010; Huang, Tian, Yu, Xu, & Feng, 2009).

Few reports are available on the fabrication of composite hydrogels based on HPMC and a high content (60% (w/w)) of micron-sized BCP for bone tissue engineering (Dorozhkin, 2001; Grimandi, Weiss, Millot, & Daculsi, 1998; Weiss et al., 2003). However, the mechanisms governing the changes induced in the thermal gelation of HPMC in the presence of nano-sized BCP is not fully investigated.

Injectable composite hydrogels based on HPMC, as the matrix phase, and nano-sized BCP i.e. inorganic filler were prepared and their gelation mechanism was investigated as a function of the filler phase percentage and also the ratio of HAp to β-TCP in the reinforcing phase composition, by oscillatory rheometry. Two mechanisms are suggested for induction of gelation which were assessed by determination of dissolution of the ceramics ions and adding silica nanoparticles with different particle size or hydrophilicity profiles. Injectability of the formulations was also studied as a function of their composition.

2. Materials and methods

2.1. Materials

Two grades of hydroxypropyl methylcellulose (HPMC, Metolose^{TM} 90SH) with the viscosities of 4000 (M_w (g/mol): 56,500, M_n (g/mol): 38,100) and 15,000 mPa s (M_w (g/mol): 82,900, M_n (g/mol): 56,700) were obtained from ShinEtsu Chemical Co. (Tokyo, Japan). Molecular weight characteristics of the polymers were measured by gel permeation chromatography (GPC) (GFC-Shimadzu 6A, Japan) equipped with a differential refractive index detector. The instrument was calibrated using dextran standards. The mobile phase was deionized water running at a flow rate of 1 mL min^{-1}. Diammonium hydrogen phosphate (DAHP), calcium nitrate tetrahydrate (CNTH) and ammonium hydroxide were purchased from Merck Chemicals Co. (Darmstadt, Germany). Rod-like hydroxyapatite particles (Diameter < 100 nm, aspect ratio 2–3) were purchased from Nanoshel Co. (Panchkula, India), Fig. 2a. Hydrophobic silica nanoparticles (H20, primary particle size = 10 nm, specific surface area = 170–230 m^2 g^{-1} at 20 °C, ρ = 2.2 g cm^{-3}) and hydrophilic silica nanoparticles (N20, primary particle size = 10 nm, specific surface area = 170–230 m^2 g^{-1}, ρ=2.2 g cm^{-3} at 20 °C) were supplied by Wacker Chemie AG (Germany). Hydrophilic OX50 silica nanoparticles (primary particle size = 40 nm, specific surface area = 50 ± 15 m^2 g^{-1}, ρ = 2.2 g cm^{-3} at 20 °C) were purchased from Evonik Industries (Wesseling, Germany). All chemicals were of reagent or analytical grades and used as received without further purification.

2.2. Preparation of solutions

DAPH (0.65987 g) and CNTH (1.7706 g) were dissolved separately in 100 mL of deionized water at room temperature to obtain 0.05 M clear solutions, respectively.

Table 1
Formulations for rheological property and injectability investigations and the maximum injection force.

	β-TCP (wt%)	HAp (wt%)	Maximum injection force (N)
TH-0010	0	10	3.0 (0.7)*
TH-1000	10	0	2.2 (0.2)
TH-1505	15	5	4.9 (1.6)
TH-0515	5	15	2.0 (0.8)
TH-1010	10	10	5.8 (0.5)
TH-1020	10	20	3.3 (0.7)
TH-2010	20	10	3.3 (0.4)
TH-2020	20	20	5.5 (1.2)

* The numbers in the parentheses indicate standard deviations.

HPMC solution (2% (w/w)) was prepared by dissolving an appropriate weight of the polymer in deionized water under stirring for 48 h at room temperature. The preparation details of stimulated body fluid (SBF) solution is reported elsewhere (Kokubo & Takadama, 2006).

2.3. Methods

2.3.1. Synthesis and characterization of β-TCP nanoparticles

Plate-like β-TCP nanoparticles were synthesized via a wet-chemical method. To this end, CNTH (0.075 M) solution was added dropwise (rate = 0.7 mL min^{-1}) to DAHP (0.05 M) solution under vigorous agitation. The DAHP (0.05 M) solution temperature was maintained at 33 °C before addition. pH of the resulting solution was adjusted at 7.3 by adding an appropriate amount of ammonium hydroxide solution. After a while, the solution became opaque, and started to precipitate. After agitation for 24 h, the precipitate was then filtered and dried at 80 °C for 24 h. The dried precipitate was calcinated at 800 °C for 5 h with a heating and cooling rate of 5 °C min^{-1}.

β-TCP nanoparticles were characterized by X-ray diffraction (XRD, D5000 Diffraktometer, Siemens, Germany) using an FK 60-04 air insulated X-ray diffraction tube with Cu $K\alpha$ radiation anode working at 1500 V. The experiments were performed using monochromated Cu $K\alpha$ radiation in the 2θ range between 5° and 70° at 25 °C. Morphology and particle size and size distribution of the synthesized nanoparticles were assessed using a scanning electron microscope (SEM, VEGA, TESCAN, Czech Republic) after sputter-coating with a thin layer of gold.

2.3.2. Preparation of nanocomposite gels

To investigate the effect of inorganic phase on the rheological behavior and injectabilty of the resulting nanocomposite gels, formulations were prepared with varying inorganic phase content and its composition. The composites were prepared by mixing the HPMC solution (2% (w/w)) with the mineral phase and consequent homogeniztion (DIAX900, Heidolph, Germany) at 26,000 rpm for 2 min. The composition of the formulations is tabulated in Table 1.

2.3.3. Rheological measurements

The rheological measurements were conducted using a MCR300 (Anton Paar, Graz, Austria) rheometer utilizing parallel plate measuring geometry (25 mm in diameter and 1 mm gap). Experiments were performed based on a temperature ramp from 25–90 °C (for HPMC solutions) and 10–70 °C for HPMC solutions containing ceramic phase at a fixed heating rate of 2 °C min^{-1} and frequency of 1 Hz. Linear viscoelastic regions were previously determined for all formulations by performing strain sweep (0.00994–300%) tests.

Steady rheology tests were considered to follow the likely shear-induced breakdown of the structure during injection conditions. These tests were performed at 25 °C with a shear rate range of 0.01–1000 s^{-1}.

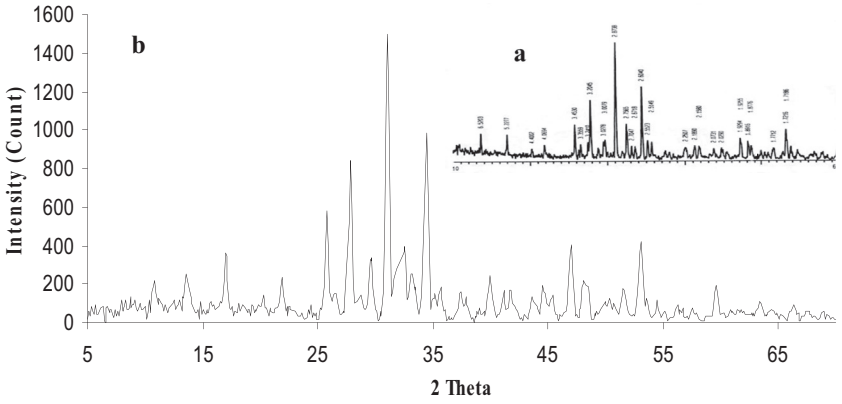

Fig. 1. (a) Standard X-ray diffraction pattern of β-TCP, and (b) synthesized β-TCP.

2.3.4. Injectability

Injectability test was performed at ambient temperature (25 °C) by a universal testing machine (STM-20, Santam, Iran) using a 5 mL syringe (d = 13 mm, and $d_{orifice}$ = 1.2 mm). The mixture was charged into the syringe after homogenization (Heidolph, DIAX900, Germany) for 2 min. The syringe was assembled between the compression plates of the universal testing machine using a home-made assembly and compression was applied on the syringe

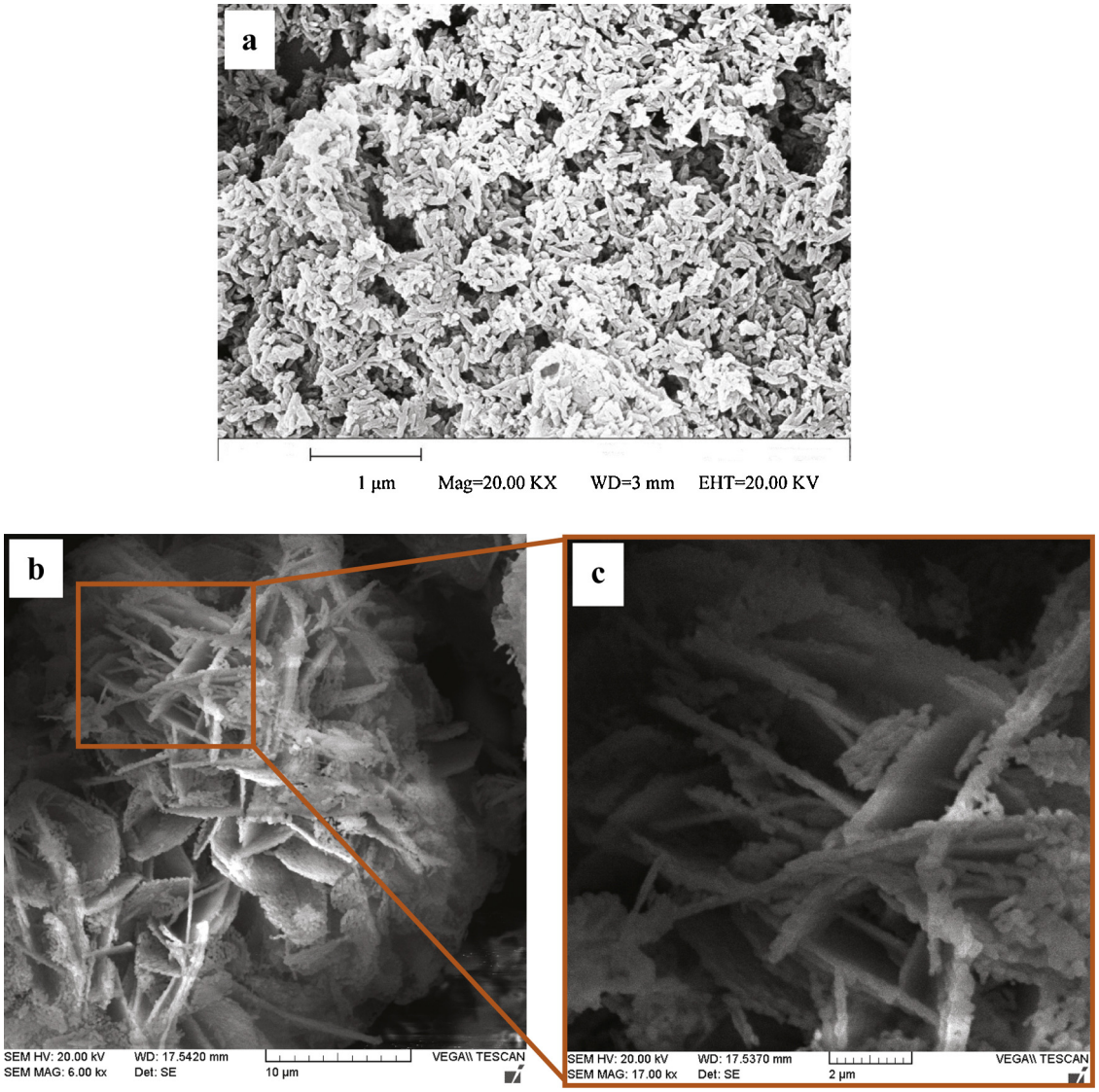

Fig. 2. SEM micrographs of (a) commercially available HAp (provided by Nanoshel Co. (Panchkula, India)), and (b) synthesized β-TCP. The inset (c) shows the β-TCP at higher magnification. The average thickness of the platlets based on 20 measurements is 98 nm (standard deviation = 3 nm).

plunger at a crosshead speed of 15 mm min^{-1}. A maximum limit of 100 N was chosen for the test because higher forces are not practical in manual injection during surgery (Ginebra et al., 2001; Khairoun, Boltong, Driessens, & Planell, 1998; Xu et al., 2006). The injection force at the plateau region was recorded as the injectability force.

2.3.5. Bioresorbability and pH determination

Bioresorbability of the nanocomposite hydrogel scaffolds was evaluated using homogenized specimens (W = 200 mg, 10% (w/w) BCP:HPMC) as previously described for the injectability test. The specimens were inserted separately into dialysis bags which were then soaked in 40 mL of SBF later on. The calcium ions dissolved in the SBF medium was determined by atomic absorption spectrometry (AAS-Spectra AA-100, Varian, Australia) within pre-determined immersion periods of 1, 2, 3, 4 week.

The injectable nanocomposite scaffolds (W = 200 mg) were also charged in polyethylene terephthalate (PET) bottles containing 40 mL of SBF solution and incubated (Incucell, MMM Medcenter Einrichtungen GmbH, Germany) in SBF (pH = 7.4) at 37 °C. The changes in the pH of SBF solution were monitored at predetermined time intervals using a pH meter (WTW, Inolab, Germany).

2.4. Data analysis

Statistical analyses were performed using analysis of variance (ANOVA) and Tukey's post-hoc test. Differences were considered statistically significant when the p value was < 0.05.

3. Results and discussion

3.1. Synthesis of the mineral phase

X-ray diffraction profiles of the calcined powders confirmed the formation of the β-TCP phase (Fig. 1) with the characteristic peaks similar to the JCPDS (Joint Committee on Powder Diffraction Standards) card number 09-0169. SEM micrographs of the commercially available HAp and synthesized β-TCP are shown in Fig. 2, in which a plate-like structure with a thickness of 100–200 nm for the synthesized β-TCP is observed (Fig. 2b).

3.2. Rheological properties of neat polymers

Effect of temperature on gelation of two HPMC aqueous solutions was studied by oscillatory tests. Comparison of the rheological results for HPMC1 with HPMC2 (Fig. 3) shows that the gelation temperature of HPMC1 is lower than that of HPMC2. The gelation temperature is considered as the temperature at which the viscosity is dramatically increased (Silva et al., 2008).

HPMC1 which has a low molecular weight and a rod-like structure aggregates more easily via a parallel arrangement along the chain than the high molecular weight polymer that has a random coil configuration (Sarkar, 1979), and therefore its hydrophobic interaction starts earlier and gelation temperature is reduced. Sarkar (1979) proposed this phenomenon for the observed lower cloud point of methylcellulose with lower molecular weight. The final G' and complex viscosity of HPMC2 is also higher than that of HPMC1, because of its higher molecular weight.

As the aim of this study was preparation of an in-situ forming scaffold, the HPMC with lower gelation temperature (HPMC1) was chosen for further investigations. The gelation temperature of HPMC1, however, is still higher than the physiological temperature, which can be lowered by incorporation of the mineral phase along with HPMC.

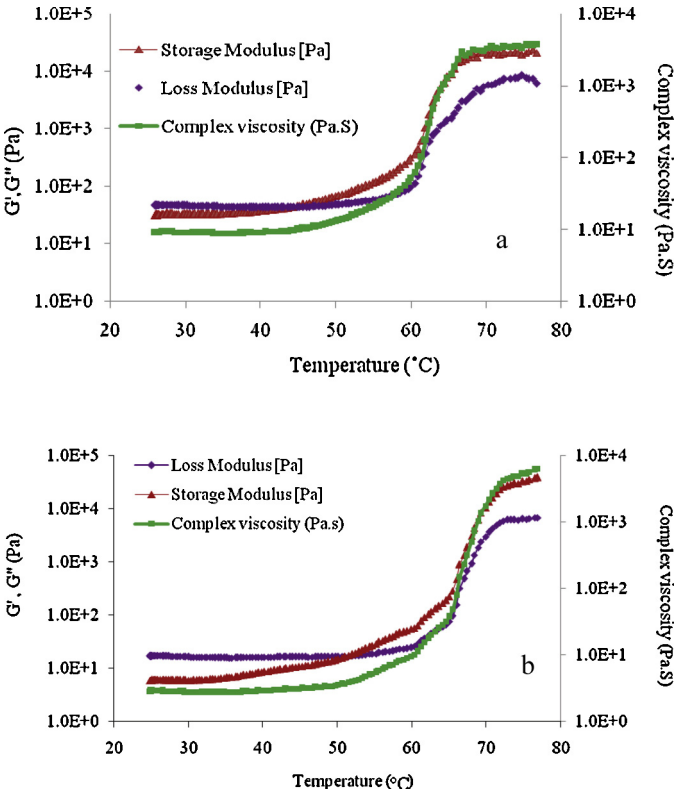

Fig. 3. Storage modulus (G'), loss modulus (G'') and complex viscosity as a function of temperature in (a) 2 wt% HPMC1 solution and (b) 2 wt% HPMC2 solution.

3.3. Composite hydrogels

3.3.1. Dynamic rheological measurements

In the dynamic rheology, an oscillatory strain is applied and viscous and elastic properties of the sample are simultaneously measured.

As illustrated in Figs. 4 and 5, the increase in mineral phase content results in a corresponding increment in viscosity and G', and, at the same time, a reduction in the incipient gelation temperature. Increasing viscosity and G' can be attributed to the reduction in free volume between chains (Shenoy, 1999). The curves also show that formulations with high mineral phases (30 and 40 wt%) are less temperature sensitive, because with increasing the minerals, the phase which is not temperature sensitive, would be dominant in the system. Thus, the specimens containing 10–20 wt% mineral phase are more temperature sensitive and suitable for preparing the in-situ forming scaffolds (Fig. 5).

As can be seen in Fig. 5, G' and viscosity gradients are higher for specimens, TH-1000, TH-1505 and TH-1010. Therefore, these formulations are suggested for possible preparation of temperature-sensitive in-situ forming scaffolds. However, because of the low injection force of TH-1000 (Table 1), it is preferred to TH-1505 and TH-1010. The formulation also provides higher possibility for cell infiltration and oxygen, nutrients and other water-soluble metabolites permeability.

Nano-HAp particles agglomerate due to their high surface area (Shenoy, 1999). The formulations with higher β-TCP content showed higher viscosity. This might be because of plate-like morphology of β-tricalcium phosphate which dissipates energy due to the friction of the particles upon rotation (Ferguson & Kemblowski, 1991). Complex viscosity and G' of the TCP-containing specimens increase sharply and gelation temperature is reduced more than the other formulations. Reduction in gelation temperature might be due to the new interactions formed between HPMC chains and

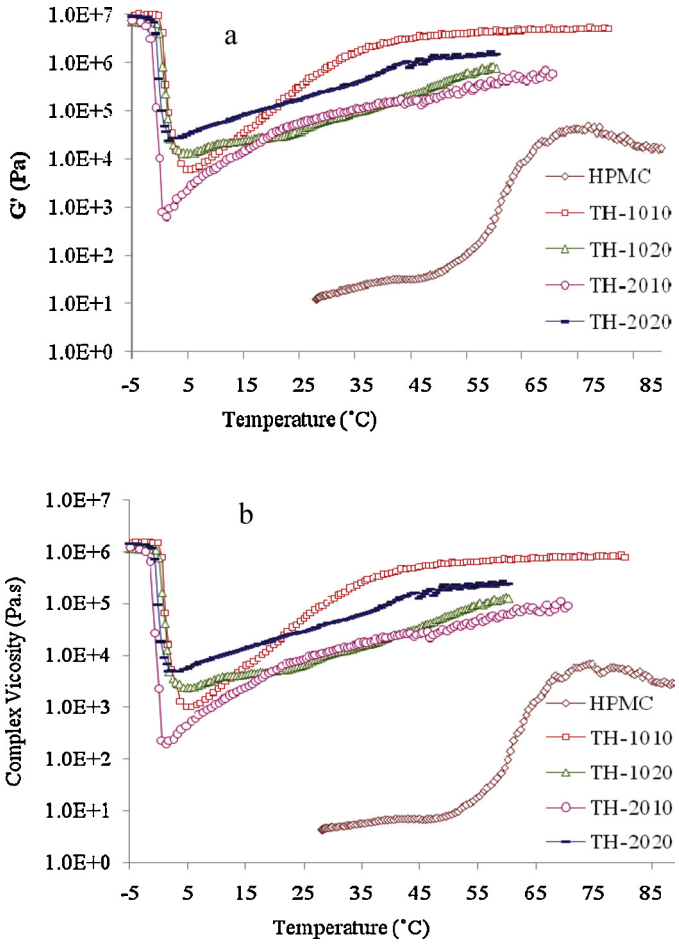

Fig. 4. (a) Storage modulus (G') and (b) complex viscosity variations with increasing temperature for HPMC and biphasic calcium phosphate specimens with different mineral phase ratios.

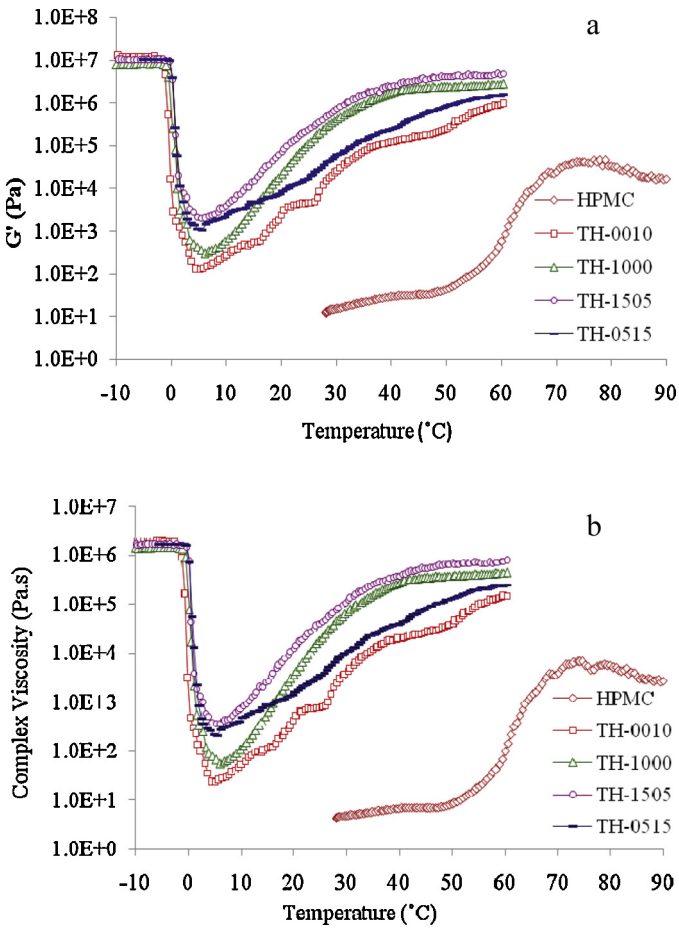

Fig. 5. (a) Storage modulus (G') and (b) complex viscosity variations with increasing temperature for HPMC and biphasic calcium phosphate specimens with different mineral phase ratios.

the mineral phase and between HPMC chains and ions released from the mineral phase.

To investigate the nature of any interaction mechanism, silica nanoparticles having no ionic entity release were used as nanofillers to reflect only particle interaction with polymeric matrix.

Adding ionically inert but hydrophobic silica (H20) nanoparticles, it was found that G', G'' and viscosity of the gels were increased and gelation temperature reduced with respect to temperature in the temperature sweep rheograms as shown in Fig. 6. Increase in G', G'' and the viscosity of the gels can be attributed to the increase in solution-state miscibility of HPMC and silica H20 nanoparticles. On increasing the temperature, the HPMC solution gels due to the hydrophobic interactions occurring after changing the solvation state of the hydrophobic segments of the polymer chain. Therefore, the observed reduction in gelation temperature for silica H20-containing specimens can be attributed to the role of these particles as (hetro)nuclei for hydrophobic aggregation.

Temperature–sweep rheograms for dispersions containing HPMC and hydrophilic silica nanoparticles (Silica N20; silanol activity $\approx$2 SiOH nm^{-2}) is also shown in Fig. 6. It is expected that this nanofiller should exhibit strong interactions due to hydrogen bonds with HPMC hydroxyl groups. These new interactions are so strong that they suppress hydrophobic interactions (even up to 60 °C) showing no gelation and behavior independent of temperature.

Silica OX50 nanoparticles are hydrophilic, but having lower surface area and larger particle size ($50 \pm 15\,m^2\,g^{-1}$ comparing to 170–230 $m^2\,g^{-1}$ for silica N20). Therefore, the potential for providing hydrogen bonds is significantly lower than for silica N20. As observed in Fig. 6, HPMC specimens containing silica OX50 nanoparticles exhibit the presence of hydrophobic interactions firstly, then a reduction in the gelation temperature probably due to the occurrence of hydrogen bond-interactions at about 30 °C. The lack of hydrophobic interactions resulted in the temperature independency of G', G'' and viscosity.

Rheological studies of silica nanoparticles (H20, N20 and OX50) revealed that hydrophilicity, hydrophobicity, surface area and size of particles affect the rheological properties of HPMC gels.

3.3.2. Steady rheological measurements

In order to improve injectability of the in-situ forming scaffolds, reduced viscosity upon applied injection shear force (i.e. pseudoplast behavior) is desirable.

As shown in Fig. 7, the formulations are shear-thining and the specimens with higher mineral phase have higher viscosity. When the filler concentration is increased: (i) The number of particles per unit volume which comes in contact during the increase of the flow. Several models have been proposed to predict the viscosity of dilute suspensions. In most of the models the volume fraction of the dispersed phase is the main parameter determining the viscosity of the suspension. For example, the Einstein equation, which is one of the earliest and simplest models, predicts the viscosity of a dilute suspension as follows (Nielsen & Landel, 1994):

$$\eta_s = \eta_m(1 + 2.5V_f)$$

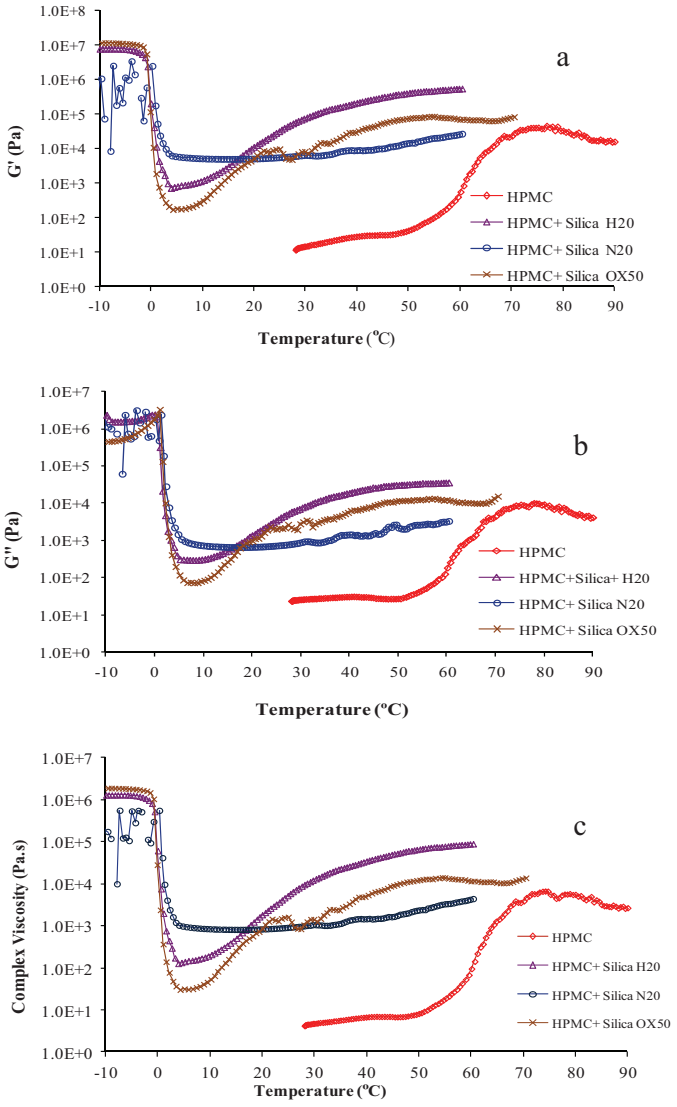

Fig. 6. (a)Storage modulus (G'), (b) loss modulus (G''), (c) complex viscosity variations with increasing temperature for neat HPMC and nanocomposite specimens containing silica H20, silica N20 and silica OX50.

where η_s, η_m, and V_f are the viscosity of the suspension and matrix, and volume fraction of solid particles, respectively.

(ii) The interparticle attraction and repulsion effects become stronger due to electrostatic charges, which depend upon the polarity of the medium, and (iii) the rotation of the particles during flow, as well as the formation of doublets and their rotation during flow, produces additional dissipative effects which lead to an increase in the viscosity (Shenoy, 1999). The formulation with higher β-TCP shows higher viscosity. This might be due to the plate-like morphology of β-TCP which provides additional dissipation upon rotation.

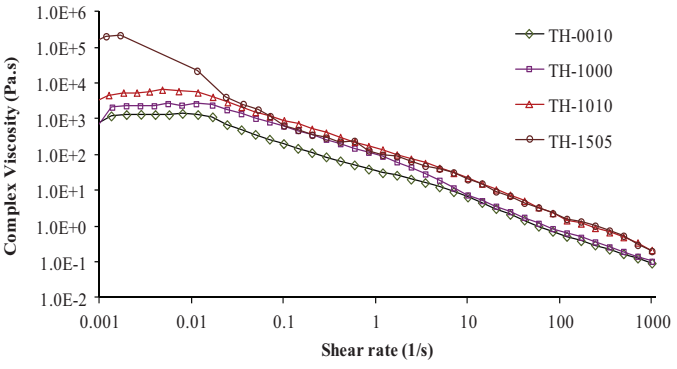

Fig. 7. Viscosity versus shear rate behavior for specimens with different mineral phase composition.

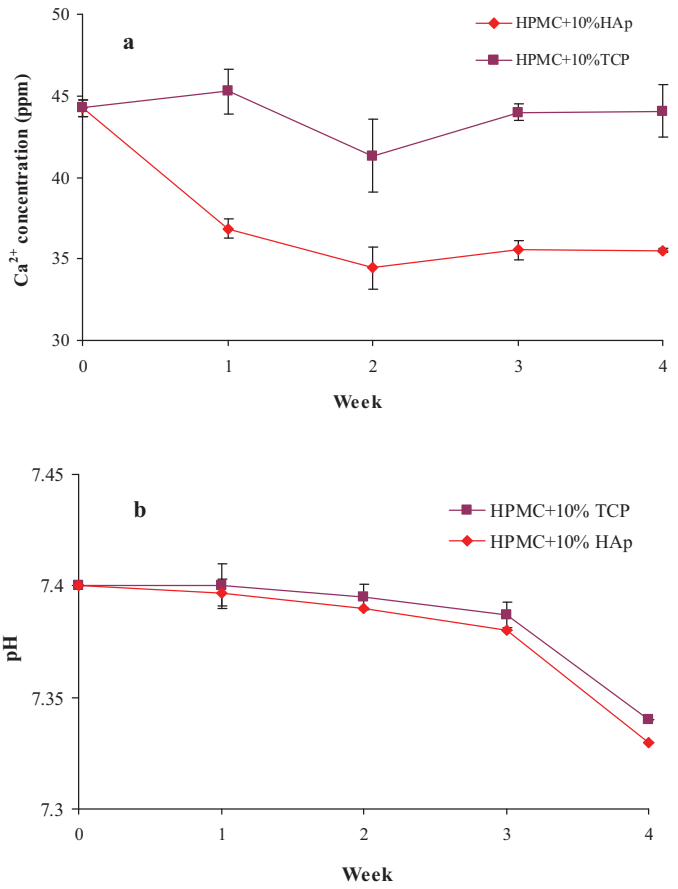

Fig. 8. Variation of (a) calcium content (ppm) and (b) pH vs. soaking time in SBF for hydrogels containing 10% HAp and 10% β-TCP.

3.3.3. Injectability

The forces at the plateau region for different groups are shown in Table 1. All formulations were completely injectable and the injection force for TH-1010, TH-1505 and TH-2020 were higher in comparison with the other formulations indicating that the injection force increased with increasing modulus and viscosity at room temperature.

3.3.4. In vitro bioresorbability and pH evaluations

To elucidate the interactions between the mineral phase and HPMC and the effect of ion release on rheological behavior of the scaffold, bioresorbability of TH-1000 and TH-0010 in SBF solution were investigated. As Fig. 8 depicts the immersion of the scaffolds in SBF solution induces changes in Ca^{2+} concentration. A remarkable reduction in Ca^{2+} concentration is seen in the specimen containing 10% HAp, extending to the second week. This is due to the surface uptake of Ca^{2+} and PO_4^{3-} and formation of a new apatite-like phase on the surface of the HAp scaffold. The pH reduction in this period of time also confirms PO_4^{3-} consumption due to apatite formation. After the second week there is no statistically significant difference in Ca^{2+} concentration which could be attributed to a balance between uptake of the Ca^{2+} and dissolution of the Ca^{2+} of the scaffold.

There is no significant difference between the calcium ions concentration in the SBF solution in the case of specimens containing β-TCP ($p > 0.05$), which might be due to high resorbability of β-TCP. Therefore there is a balance between the release of the Ca^{2+} into the SBF and the formation of apatite on the surface of scaffold. The decrease in pH up to the fourth week is probably due to the PO_4^{3-} consumption and apatite formation.

4. Conclusion

In-situ forming, injectable temperature-sensitive calcium phosphate containing composite scaffolds were formulated using HAp and β-TCP as the mineral dispersed phase and HPMC as the matrix. Results showed that the incorporation of HAp and β-TCP nanoparticles in the HPMC aqueous solution increases G', G'' and viscosity of the injectable scaffolds, but decreases the gelation temperature. The formulations with low mineral phases are more temperature-sensitive because of the high temperature-sensitive polymer content. These formulations also provide high injectability. Formulations with high β-TCP content (especially TH-1000) are more temperature sensitive with low injection forces, therefore, are more suitable for preparing in-situ forming scaffolds. The mechanism of nanofiller–polymer interactions was examined by substituting the nanofiller phase by silica H20, N20 and OX50 nanoparticles, which proved that any interaction (hydrophobic or hydrophilic) between nanoparticles and HPMC affects the rheological behavior of the scaffolds. Use of bioresorbability tests showed that salting-out effect of ions released from the mineral phase plays a significant role in gelation behavior of HPMC. Potential dental and craniofacial uses of the improved scaffolds include mandibular and maxillary ridge augmentation, and socket preservation after extraction. Other potential uses could be the support of metal dental implants or augmentation of deficient implant sites.

Appendix A. Supplementary data

Supplementary data associated with this article can be found, in the online version, at http://dx.doi.org/10.1016/j.carbpol.2013.07.078.

References

Boix, D., Weiss, P., Gauthier, O., Guicheux, J., Bouler, J. M., Pilet, P., et al. (2006). Injectable bone substitute to preserve alveolar ridge resorption after tooth extraction: A study in dog. *Journal of Materials Science Materials in Medicine*, *17*(11), 1145–1152.

Castellani, C., Zanoni, G., Tangl, S., Van Griensven, M., & Redl, H. (2009). Biphasic calcium phosphate ceramics in small bone defects: Potential influence of carrier substances and bone marrow on bone regeneration. *Clinical Oral Implants Research*, *20*(12), 1367–1374.

Cho, J. S., Jung, D. S., Han, J. M., & Kang, Y. C. (2009). Nano-sized α and β-TCP powders prepared by high temperature flame spray pyrolysis. *Materials Science and Engineering: C*, *29*(4), 1288–1292.

Damien, C. J., & Parsons, J. R. (1991). Bone graft and bone graft substitutes: A review of current technology and applications. *Journal of Applied Biomaterials*, *2*(3), 187–208.

De Boever, J. A., De Boever, A. L., & De Vree, H. M. (1998). Periodontal aspects of cementation: Materials, technics and their biologic reactions. *Revue Belge de Médecine Dentaire t*, *53*(4), 181–192.

Dorozhkin, S. V. (2001). Is there a chemical interaction between calcium phosphates and hydroxypropylmethylcellulose (HPMC) in organic/inorganic composites? *Journal of Biomedical Materials Research*, *54*(2), 247–255.

Dorozhkin, S. V. (2010a). Calcium orthophosphates as bioceramics: State of the art. *Journal of Functional Biomaterials*, *1*(1), 22–107.

Dorozhkin, S. V. (2010b). Nanosized and nanocrystalline calcium orthophosphates. *Acta Biomaterialia*, *6*(3), 715–734.

Escudero, J. J., Ferrero, C., & Jiménez-Castellanos, M. R. (2010). Compaction properties, drug release kinetics and fronts movement studies from matrices combining mixtures of swellable and inert polymers. II. Effect of HPMC with different degrees of methoxy/hydroxypropyl substitution. *International Journal of Pharmaceutics*, *387*(1-2), 56–64.

Ferguson, J., & Kemblowski, Z. (1991). *Applied fluid rheology*. London: Elsevier Applied Science.

Ginebra, M. P., Rilliard, A., Fernández, E., Elvira, C., Román, J. S., & Planell, J. A. (2001). Mechanical and rheological improvement of a calcium phosphate cement by the addition of a polymeric drug. *Journal of Biomedical Materials Research*, *57*, 113–118.

Grimandi, G., Weiss, P., Millot, F., & Daculsi, G. (1998). In vitro evaluation of a new injectable calcium phosphate material. *Journal of Biomedical Materials Research*, *39*(4), 660–666.

Huang, Z., Tian, J., Yu, B., Xu, Y., & Feng, Q. (2009). A bone-like nano-hydroxyapatite/collagen loaded injectable scaffold. *Biomedical Materials*, *4*(5), 055005.

Khairoun, I., Boltong, M. G., Driessens, F. C., & Planell, J. A. (1998). Some factors controlling the injectability of calcium phosphate bone cements. *Journal of Materials Science Materials in Medicine*, *9*, 425–428.

Kim, H. (2007). *Synthesis and control of microstructure, mechanical properties, and bioactivity in biphasic and preferentially oriented calcium phosphate bioceramics*. Thesis. University of Alabama at Birmingham, Birmingham, AL.

Kokubo, T., & Takadama, H. (2006). How useful is SBF in predicting in vivo bone bioactivity? *Biomaterials*, *27*(15), 2907–2915.

Laurencin, C. T., Ambrosio, A. M. A., Borden, M. D., & Cooper, J. A., Jr. (1999). Tissue engineering: Orthopedic applications. *Annual Review of Biomedical Engineering*, *1*, 19–46.

Lee, D. D., Tofighi, A., Aiolova, M., Chakravarthy, P., Catalano, A., Majahad, A., et al. (1999). [alpha]-BSM (R): A biomimetic bone substitute and drug delivery vehicle. *Clinical Orthopaedics and Related Research*, *367*, S396–S405.

Link, D. P. (2008). *Bone cement: biological properties of biodegradable polymeric microparticles*. UB Nijmegen.

Mickiewicz, R.A. (2001). *Polymer–calcium phosphate composites for use as an injectable bone substitute*. B.A.Sc., University of Toronto, Toronto.

Moore, W. R., Graves, S. E., & Bain, G. I. (2001). Synthetic bone graft substitutes. *ANZ Journal of Surgery*, *71*(6), 354–361.

Nielsen, L. E., & Landel, R. F. (1994). *Mechanical properties of polymers and composites* (2nd ed.). New York: Marcel Deker Inc.

Pérez, O. E., Wargon, V., & Pilosof, A. M. R. (2006). Gelation and structural characteristics of incompatible whey proteins/hydroxypropylmethylcellulose mixtures. *Food Hydrocolloids*, *20*(7), 966–974.

Weiss, P., Clergeau, L. P., Enckel, B., Amouriq, Y., Giumelli, B., Jean, A., & Daculsi, G. (2005). A new injectable bone substitute concept (MBCP Gel ™): First clinical results in human maxillo-facial surgery. *Key Engineering Materials*, *284–286*, 1053–1056.

Sarkar, N. (1979). Thermal gelation properties of methyl and hydroxypropyl methylcellulose. *Journal of Applied Polymer Science*, *24*(4), 1073–1087.

Silva, S. M. C., Pinto, F. V., Antunes, F. E., Miguel, M. G., Sousa, J. J. S., & Pais, A. A. C. C. (2008). Aggregation and gelation in hydroxypropylmethyl cellulose aqueous solutions. *Journal of Colloid and Interface Science*, *327*, 333–340.

Slaughter, B. V., Khurshid, S. S., Fisher, O. Z., Khademhosseini, A., & Peppas, N. A. (2009). Hydrogels in regenerative medicine. *Advanced Materials*, *21*(32-33), 3307–3329.

Temenoff, J. S., & Mikos, A. G. (2000). Injectable biodegradable materials for orthopedic tissue engineering. *Biomaterials*, *21*(23), 2405–2412.

Shenoy, A. V. (1999). . *Rheology of filled polymer systems* (vol. 4) The Netherlands: Springer.

Weiss, P., Obadia, L., Magne, D., Bourges, X., Rau, C., Weitkamp, T., et al. (2003). Synchrotron X-ray microtomography (on a micron scale) provides three-dimensional imaging representation of bone ingrowth in calcium phosphate biomaterials. *Biomaterials*, *24*(25), 4591–4601.

Xu, H. H. K., Weir, M. D., Burguera, E. F., & Fraser, A. M. (2006). Injectable and macroporous calcium phosphate cement scaffold. *Biomaterials*, *27*(24), 4279–4287.

Xu, H. H. K., Weir, M. D., & Simon, C. G. (2008). Injectable and strong nano-apatite scaffolds for cell/growth factor delivery and bone regeneration. *Dental Materials*, *24*, 1212–1222.

Yang, Y., Kim, K.-H., & Ong, J. L. (2005). A review on calcium phosphate coatings produced using a sputtering process—An alternative to plasma spraying. *Biomaterials*, *26*(3), 327–337.

Zhao, L., Weir, M. D., & Xu, H. H. K. (2010). An injectable calcium phosphate-alginate hydrogel-umbilical cord mesenchymal stem cell paste for bone tissue engineering. *Biomaterials*, *31*(25), 6502–6510.